Chromosome Localization Changes in the *Trypanosoma cruzi* Nucleus

M. Carolina Q. B. Elias,[1] Marcella Faria,[1] Renato A. Mortara,[1] Maria Cristina M. Motta,[2]
Wanderley de Souza,[2] Marc Thiry,[3] and Sergio Schenkman[1]*

Departamento de Microbiologia, Imunologia e Parasitologia, Universidade Federal de São Paulo, São Paulo,[1] and Laboratório de Ultraestrutura Celular Hertha Meyer, Instituto de Biofísica Carlos Chagas Filho, Universidade Federal do Rio de Janeiro, Rio de Janeiro,[2] Brazil, and Laboratory of Cellular and Tissue Biology, University of Liège, Liège, Belgium[3]

Chromosome localization in the interphase nuclei of eukaryotes depends on gene replication and transcription. Little is known about chromosome localization in protozoan parasites such as trypanosomes, which have unique mechanisms for the control of gene expression, with most genes being posttranscriptionally regulated. In the present study, we examined where the chromosomes are replicated in *Trypanosoma cruzi*, the agent of Chagas' disease. The replication sites, identified by the incorporation of 5-bromodeoxyuridine, are located at the nuclear periphery in proliferating epimastigote forms in the early S phase of the cell cycle. When the S phase ends and cells progress through the cell cycle, 5-bromodeoxyuridine labeling is observed in the nuclear interior, suggesting that chromosomes move. We next monitored chromosome locations in different stages of the cell cycle by using a satellite DNA sequence as a probe in a fluorescence in situ hybridization assay. We found two distinct labeling patterns according to the cell cycle stage. The first one is seen in the G_1 phase, in hydroxyurea-arrested epimastigotes or in trypomastigotes, which are differentiated nondividing forms. In all of these forms the satellite DNA is found in dots randomly dispersed in the nucleus. The other pattern is found in cells from the S phase to the G_2 phase. In these cells, the satellite DNA is found preferentially at the nuclear periphery. The labeling at the nuclear periphery disappears only after mitosis. Also, DNA detected with terminal deoxynucleotidyl transferase is found distributed throughout the nuclear space in the G_1 phase but concentrated at the nuclear periphery in the S phase to the G_2 phase. These results strongly suggest that *T. cruzi* chromosomes move and, after entering the S phase, become constrained at the nuclear periphery, where replication occurs.

The eukaryotic nucleus has functional compartments for DNA replication and transcription and for RNA processing (6, 24, 36). Nuclear integrity is important for DNA synthesis initiation and for replication fork formation (7), and disruption of nuclear lamina organization prevents the elongation phase of DNA replication (29). Chromosome localization in the mammalian cell nucleus is also determined by the transcriptional status of genes. Actively transcribed genes are located in the nuclear interior, replicating early in the S phase of the cell cycle, while repressed genes, which correspond to heterochromatic regions, replicate later and are located at the nuclear periphery and around the nucleolus (11, 28, 32).

Visualization of replication sites by labeling of cells with 5-bromodeoxyuridine (BrdU) or biotinylated dUTP (31) during the cell cycle revealed immobile foci probably linked to a nuclear matrix. Over the last 10 to 12 years, detailed information on the organization and dynamics of interphase chromosomes has emerged; most of them have been found associated with repeated domains, such as telomeres and centromeres (10), and related to the cell cycle (16, 26). More recently, it has been demonstrated that chromatin is highly dynamic, moving distances of >0.5 μm within seconds (8). In yeast cells this movement becomes less frequent when cells enter the S phase, and the chromosomes are retained at the nuclear periphery

(18). Similar movement constraints could occur in the nucleus of large cells, restricted to several replication units distributed in the nuclear compartment (19). Thus, it is possible that replication occurs at restricted sites and that DNA must be confined at these sites to replicate.

We decided to address this question by studying the localization of chromosome and replication sites in the nucleus of trypanosomes, because most of their genes are constitutively transcribed (21, 38) and the level of each mRNA is controlled at the posttranscriptional level (38). Therefore, chromosome localization is unlikely to be related to transcriptional regulation in these organisms, as in other eukaryotes. In addition, their nuclear structure varies during the life cycle. In epimastigotes and amastigotes, which are the replicating stages of *Trypanosoma cruzi*, the protozoan parasite that causes Chagas' disease, the nucleus is spherical and contains a large nucleolus and small amounts of heterochromatin. In contrast, in nonreplicating trypomastigote forms, the nucleus is elongated, the nucleolus disappears, and heterochromatin is found dispersed throughout the nucleoplasm (9).

Here, we studied the localization of replication sites in the nuclei of *T. cruzi* by using BrdU labeling and monitored chromosome localization by fluorescence in situ hybridization (FISH) with a satellite DNA probe (15) during different stages of the cell cycle and parasite differentiation. This probe recognizes most of the large *T. cruzi* chromosomes. We also studied the distribution of DNA content by electron microscopy after terminal deoxynucleotidyl transferase and BrdU triphosphate labeling of thin sections. We observed that the replication sites,

* Corresponding author. Mailing address: Departamento de Microbiologia, Imunologia e Parasitologia, Universidade Federal de São Paulo, R. Botucatu 862 8A, 04023-062 São Paulo, São Paulo, Brazil. Phone: 55-11-55764551. Fax: 55-11-55715877. E-mail address: sergio @ecb.epm.br.

Non-synchronized cells

Synchronized cells (BrdU pulse - 4h)

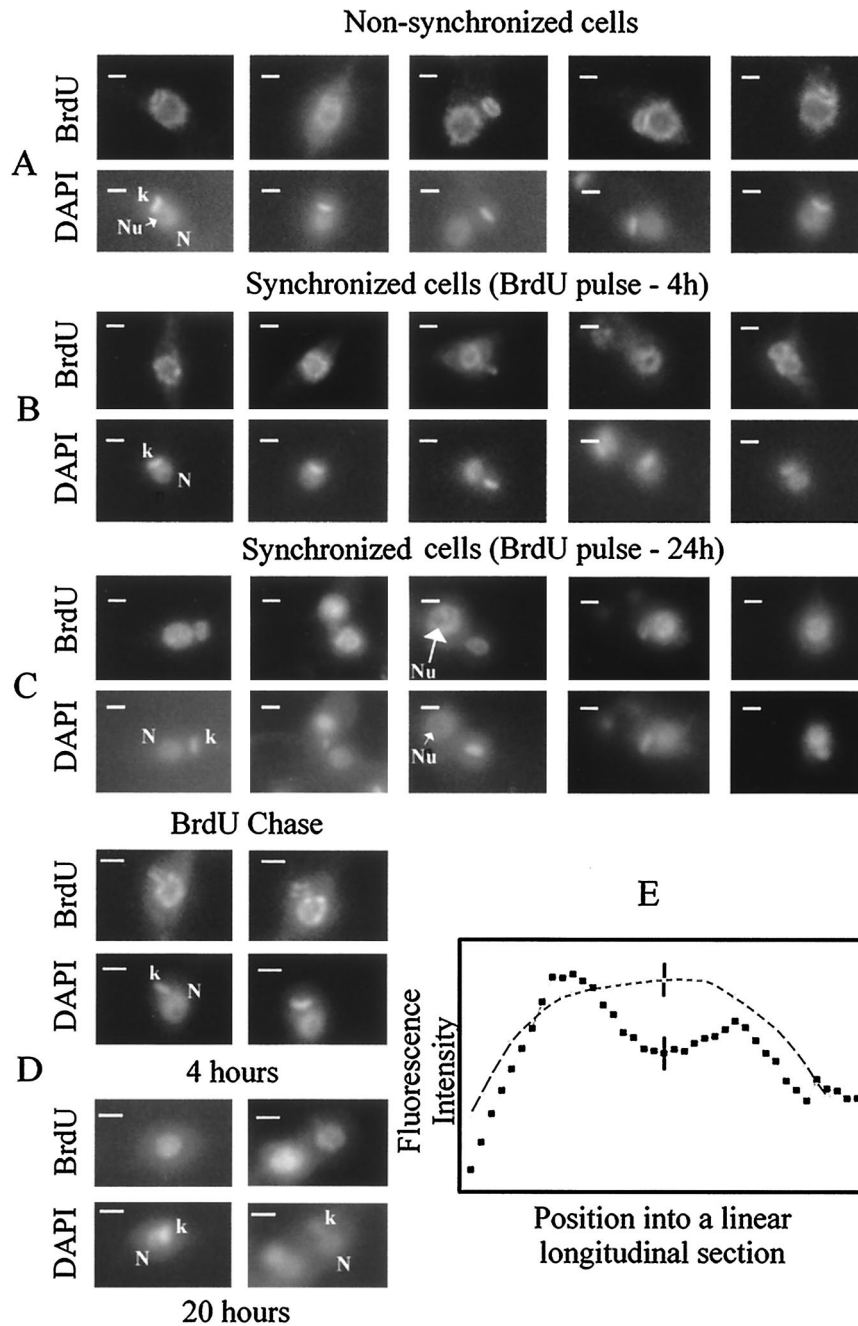## Synchronized cells (BrdU pulse - 24h)

BrdU Chase

FIG. 1. Replication sites are at the nuclear periphery of *T. cruzi*. (A) Nonsynchronized epimastigotes were incubated for 18 h. (B to D) Alternatively, epimastigotes were pretreated for 24 h with HU before incubation with BrdU for 4 h (B) or for 24 h (C), washed three times with PBS, resuspended in liver infusion tryptose medium containing 10% fetal bovine serum to chase BrdU, and maintained in cultures for different times (D). After these treatments, cells were washed, BrdU incorporation was detected by incubation with an anti-BrdU antibody followed by incubation with Cy3-conjugated anti-mouse IgG, and cells were mounted in the presence of DAPI. Images show representative examples of parasite staining. k, kinetoplast; N, nucleus; Nu, nucleolus. Bars, 1 μm. (E) The mean fluorescence intensity versus the position in a linear longitudinal section was traced over the image of each labeled nucleus of synchronized cells incubated with BrdU for 4 h ($n = 10$) (■) or for 20 h ($n = 15$) (– – –). The error bars represent the standard deviation of the mean difference between the normalized fluorescence intensities of the edges and the middle points.

the satellite DNA as well as the overall DNA, were preferentially found at the nuclear periphery during the replication phases of the cell cycle. These findings suggest that chromosomes move and become constrained at the nuclear periphery in order for replication to occur.

MATERIALS AND METHODS

Cell growth and cell cycle synchronization. *T. cruzi* epimastigote forms (strain Y) were cultured in liver infusion tryptose medium supplemented with 10% fetal bovine serum at 28°C (3). Extracellular trypomastigote forms were obtained from the supernatants of infected mammalian cells (LLCMK₂; ATCC) as described

TABLE 1. Distribution of BrdU labeling[a]

| Incorporation time | % (n) | | | Difference in labeling intensity (n)[c] |
| | Labeled parasites[b] | Nuclei with labeling | | |
		At the edge	Dispersed	
Pulse	23 ± 16 (200)	92 ± 1 (100)	8.5 ± 0.5 (100)	26 ± 9 (10)
Chase (20 h)	67 ± 3 (150)	30 ± 8 (150)	70 ± 8 (150)	1.8 ± 11 (14)

[a] The data are from the experiment shown in Fig. 1 and are given as means and standard deviations.
[b] The percentage of labeled parasites was calculated from the total number of parasites seen by DAPI staining.
[c] The relative fluorescence intensity was obtained from a line traced over each nuclear image. The fluorescence intensity was plotted against the linear section of each nucleus. The data indicate the difference in fluorescence intensity between the nuclear edge and the center of the nucleus ($P = 0.000002$) (Student's t test).

previously (1). For the synchronization experiments, epimastigote cultures were diluted to a concentration of 3×10^6 parasites per ml, and after 16 h, 20 mM hydroxyurea (HU) was added as described previously (14). After 24 h, the parasites were directly used or were washed three times with phosphate-buffered saline (PBS) and maintained in cultures in the presence or absence of BrdU for various times.

Flow cytometry analysis and FISH. Cells were washed with PBS and fixed with 50% ethanol in PBS for 10 min at 0°C. Cells were washed once more with PBS and resuspended in PBS containing 20 μg of propidium iodide per ml. Cells were then analyzed with a custom-designed flow cytometer (Becton-Dickinson Excalibur). The FISH probe was one repeat of satellite DNA obtained by digestion of genomic DNA from *T. cruzi* strain Y with *Sac*I. The 195-bp fragment obtained was cloned in the *Sac*I site of pBlueScript SK⁻ (Stratagene) (pSatTc). The sequence exactly corresponds to the sequence previously described (15).

The satellite probe was labeled with digoxigenin by PCR. A first standard PCR was performed with 40 ng of pSatTc as a template and 20 pmol of T3 and T7 primers in a final volume of 100 μl. The PCR product was analyzed on a 1% agarose gel, and the expected fragment was eluted by using a Sephaglass Band-Prep kit (Pharmacia). Ten nanograms of the eluted band was then used as a template in a second reaction with the same primers and with 0.2 mM each dATP, dCTP, and dGTP, 0.13 mM dTTP, and 0.07 mM digoxigenin-11-dUTP (Roche Diagnostics). The labeled PCR product was purified by using a QIAquick PCR purification kit (Qiagen).

Cells obtained from cultures were washed with PBS and placed on slides previously treated with 2% silane (Sigma) in acetone for 1 min. Cells were fixed with 4% *p*-formaldehyde in PBS for 25 min, washed twice (for 5 min each time) with PBS, and permeabilized with 0.1% Triton X-100 in PBS for 5 min. After another wash, the cells were postfixed with 2% formaldehyde in PBS for 10 min and washed with PBS for 5 min. Cells were dehydrated by 5-min incubations with 70, 90, and 100% cold ethanol and air dried.

One microliter of digoxigenin-labeled satellite probe was added to 25 μl of hybridization solution, which contained 2× SSPE (1× SSPE is 0.18 M NaCl, 10 mM NaH₂PO₄, and 1 mM EDTA [pH 7.7]), 50% formamide, and 10% dextran sulfate; the mixture was heated at 85°C for 7 min. The hybridization solution was added to the cells, and the slides were sealed with EasiSeal (Hybaid) and heated at 100°C for 5 min for denaturation of target and probe DNAs. Hybridization was performed overnight at 37°C. Slides were washed with 2× SSC (1× SSC is 0.15 M NaCl plus 0.015 M sodium citrate)– 50% formamide for 30 min at 37°C, 2× SSC for 10 min at 50°C, 0.2× SSC for 50 min at 50°C, and 4× SSC for 10 min at room temperature. Labeling was detected by incubating slides with sheep antidigoxigenin (30 ng per ml) (Roche) diluted in PBS– 1% bovine serum albumin (BSA) for 45 min at 37°C. After two washes (5 min each time) with Tris-buffered saline– 0.5% Tween 20, the slides were incubated with fluorescein-conjugated anti-sheep antibody (10 μg per ml) (Vector) diluted in PBS– 1% BSA for 45 min at 37°C. Slides were washed again and mounted in Vectashield (Vector) in the presence of 10 μg of 4′,6′-diamidino-2-phenylindole (DAPI) per ml.

Images were acquired (i) with the Leica Qwin program by using an ADIMEC MX12P camera attached to a Nikon Optiphot-2 epifluorescence microscope equipped with a ×100 Fluor 100/1.3 oil objective or (ii) with the LaserSharp 3.2TC program (Bio-Rad) by using the Zeiss ×100/1.4 Plan-Apochromatic lens of an Axiovert 100 microscope attached to a confocal laser fluorescence scanning system (Bio-Rad 1024-UV).

BrdU labeling. For BrdU incorporation, cells were diluted to 3×10^6 per ml of culture medium; after 8 h, 0.1 mM BrdU was added. Alternatively, cells were treated with HU for 24 h and washed or not washed with PBS three times; then, 0.1 mM BrdU was added. After 4 or 24 h, cells were collected, washed to remove BrdU from the cultures, and maintained in cultures for different times. Cells were washed three times with PBS, added to a slide containing 0.1% polylysine, fixed with cold methanol for 10 min at room temperature, and treated with 1.5 M HCl for 30 min at room temperature to expose the BrdU. Parasites were then incubated with a mouse anti-BrdU monoclonal antibody (2.5 μg per ml) (Roche) diluted in PBS– 1% BSA for 45 min at room temperature, followed by incubation with Cy3-conjugated anti-mouse immunoglobulin G (IgG) (Sigma) diluted 1:100 in PBS– 1% BSA for 45 min at room temperature. Slides were mounted in Vectashield in the presence of 10 μg of DAPI per ml. Images were acquired with the Leica Qwin program.

Electron microscopy preparations. Epimastigote forms of *T. cruzi* were fixed in 0.1% glutaraldehyde– 4% paraformaldehyde– 0.2% picric acid in 0.1 M cacodylate buffer (pH 7.2). Free aldehydes were quenched with 50 mM ammonium chloride, and the specimens were dehydrated in 30 to 90% methanol and embedded in Lowicryl K4M resin at −20°C. The ultrathin sections obtained were collected on nickel grids and, after immunocytochemical procedures, were stained with 5% (wt/vol) aqueous uranyl acetate-lead citrate.

Immunocytochemical procedures for DNA detection. The terminal deoxynucleotidyl transferase (TdT)-immunogold method was used for the localization of DNA. Grids containing thin sections were floated for 10 min at 37°C in 20 μM BrdU triphosphate (Sigma)–100 mM sodium cacodylate (pH 7.2)–2 mM MnCl₂– 10 mM β-mercaptoethanol– 50 μg of BSA per ml–calf thymus TdT (125 U per ml) (Boehringer Mannheim) (39). The sections were incubated for an additional 10 min at 37°C in the same solution supplemented with 4 μM each dCTP, dGTP, and dATP. Then, the sections were rinsed twice in double-distilled water, incubated for 30 min in PBS containing normal goat serum diluted 1:30 and 1% BSA, and rinsed with PBS– 1% BSA. Subsequently, the sections were incubated for 4 h at room temperature with the anti-BrdU monoclonal antibody diluted 1:50 in PBS–1% BSA and normal goat serum diluted 1:50. After being washed with PBS– 1% BSA, the sections were incubated at room temperature for 1 h with goat anti-mouse IgG coupled to colloidal gold (diameter, 5 to 10 nm; Jansen Life Science) and diluted 1:40 in PBS–0.2% BSA (pH 8.2). After being washed with PBS– 1% BSA, the sections were rinsed with deionized water.

Some controls were used in order to eliminate any possibility of nonspecific labeling. First, TdT or labeled nucleotides were omitted from the TdT incubation medium. Second, BrdU triphosphate was replaced with BrdU monophosphate. Third, sections were preincubated at 37°C for 2 h with 1 mg of DNase per ml in PBS– 7 mM MgCl₂. In the fourth control, sections were preincubated at 37°C for 2 h with pyrimidine-specific RNase (1 mg per ml) (Boehringer Mannheim) in 10 mM Tris-HCl (pH 7.4)–15 mM NaCl. In the fifth control, the primary antibody was omitted. Finally, the sections were incubated with antibody-free gold particles.

Pulsed-field gel electrophoresis. Agarose blocks containing gDNA were subjected to gel electrophoresis was performed with a Gene Navigator System (Amersham Pharmacia Biotech) on 1.2% agarose gels at 13°C in 0.5× Tris-borate-EDTA buffer as described previously (4). Gels were transferred to nylon membranes and hybridized with satellite or telomere probes (13) labeled by random priming.

RESULTS

The BrdU incorporation assay showed replication sites at the nuclear periphery. To study chromosome movements related to replication, we started investigating the relative locations of possible replication sites in *T. cruzi*. We incubated
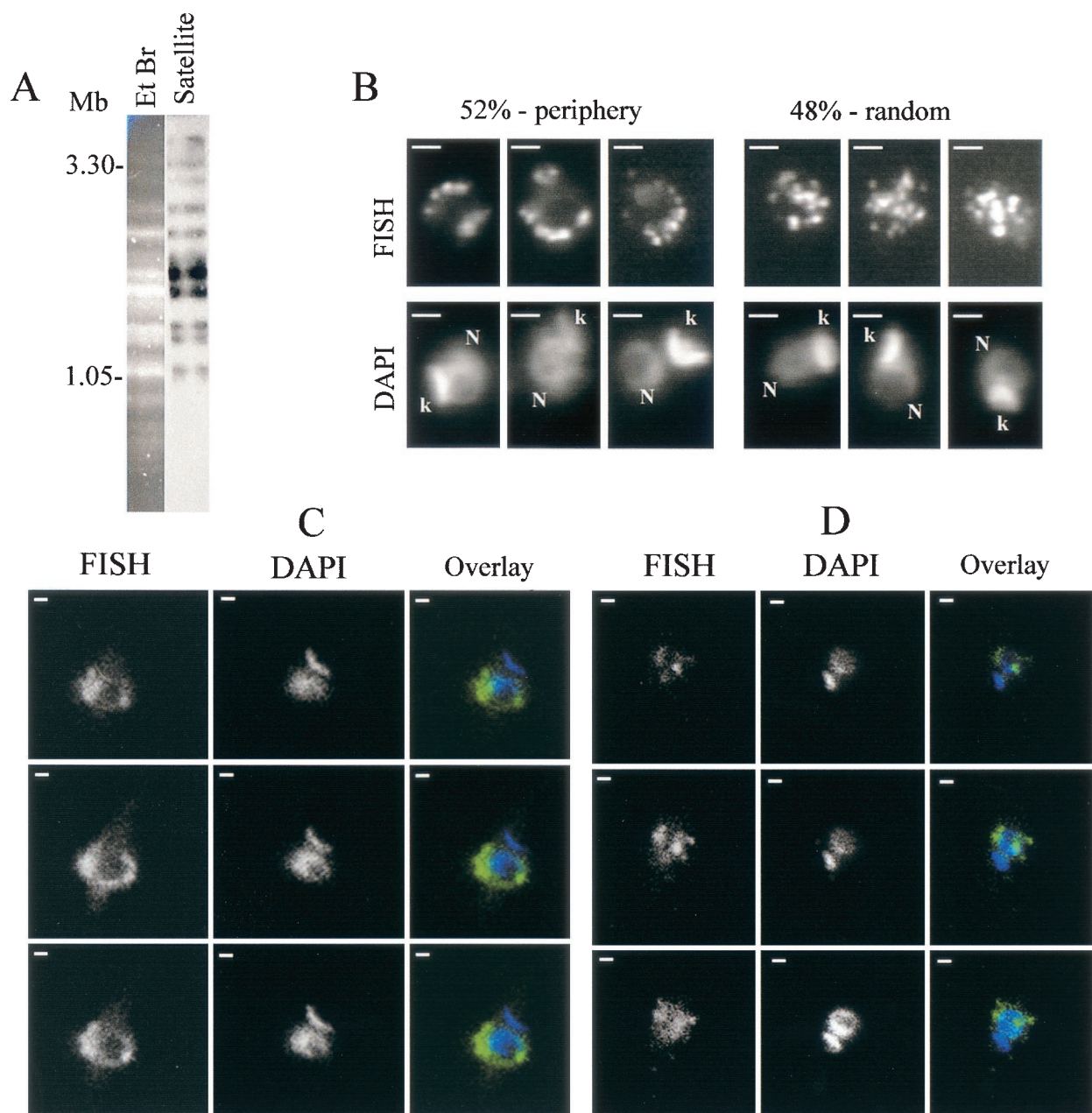
FIG. 2. There are two patterns of chromosome localization in replicative forms. (A) *T. cruzi* chromosomes were separated by pulsed-field gel electrophoresis, stained with ethidium bromide (Et Br), transferred to a nylon membrane, and hybridized with a satellite probe. The sizes of standards are indicated to the left of the gel. (B) The satellite probe labeled with digoxigenin was used to probe epimastigotes. Images show representative examples of FISH and DAPI staining. The numbers above each set of images correspond to the percentages of the patterns (peripheral and random) observed in 200 cells. N, nucleus; k, kinetoplast. (C and D) Peripheral (C) and random (D) patterns of chromosome localization were confirmed by confocal analysis of FISH assay results. In the overlay, DAPI staining is shown in blue and FISH is shown in green. Both patterns were observed in sections acquired at 0, 0.2, and 0.7 μm (from top to bottom) relative to the top section. Bars, 1 μm.

exponentially growing and nonsynchronized epimastigote forms with BrdU. As shown in Fig. 1A, labeling appeared after 18 h, mainly at the nuclear periphery (Fig. 1A), and no nuclear labeling could be detected with shorter incubation times. This long lag to label DNA synthesis occurred because high concentrations of BrdU (0.1 mM), necessary to obtain visible labeling, inhibited DNA synthesis and cell growth (data not shown). This inhibition was due to unbalancing of the de-

oxynucleoside triphosphate pool (20), as much lower [^{3}H]thymidine concentrations (1 μM) were incorporated earlier (data not shown). This effect could be reversed by the addition of equimolar amounts of deoxycytidine. Under those conditions, labeling was detected in about 20% of the cells after 2 to 4 h of incubation, occurring predominantly at the nuclear periphery. Interestingly, *T. brucei* fixed at the S phase incorporates BrdU at the periphery (40). These results provide evidence that in
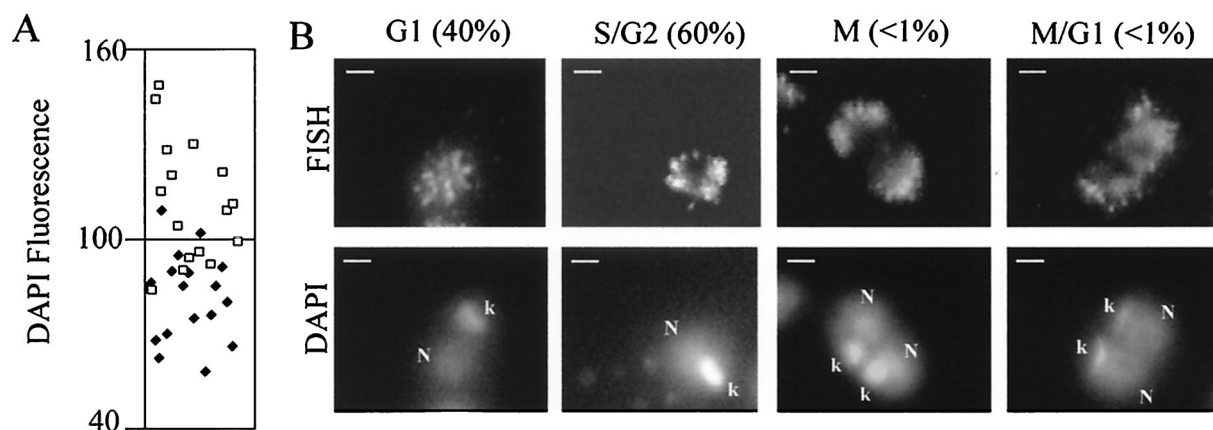
FIG. 3. Chromosomes redistribute during the *T. cruzi* cell cycle. Exponentially growing epimastigotes were subjected to FISH analysis with the satellite probe. (A) Dispersion of DAPI fluorescence intensity. Qwin software was used to measure DNA contents for the dispersed (♦) and peripheral (□) patterns of satellite FISH distribution. Images in which the nucleolus and the kinetoplast overlapped were not considered. (B) Typical images of G_1, S/G2, M, and M/G_1 phases acquired at the same settings. The numbers at the top indicate the percentages of the total numbers of parasites at the corresponding stages, as detected by DAPI quantification. The FISH patterns correspond to 18 of 29 images in G_1, 8 of 12 in S/G_2, 7 of 11 in M, and 11 of 13 in M/G_1. N, nucleus; k, kinetoplast. Bars, 1 μm.

trypanosomes, the first site where replication occurs is the nuclear periphery.

To clearly identify the locations of the replication sites, we used cells entering the S phase of the cell cycle by synchronizing the parasite cultures with HU treatment. HU is an inhibitor of ribonucleotide reductase, depleting deoxyribonucleotide pools and inhibiting DNA replication in the early S phase (42), and has been successfully used to synchronize the DNA synthesis of *T. cruzi* (12). After 2 h of incubation with BrdU, weak nuclear labeling was detected (data not shown), while clear labeling was seen after 4 h in about 30% of the cells (Fig. 1B). The reasons for this delayed BrdU incorporation were unclear, but a similar lag for [³H]thymidine incorporation was also observed under the same conditions. At 2 h after HU release, only 5% of the thymidine was incorporated, in contrast to about 25% incorporation obtained after 4 h (data not shown). Ninety percent of the BrdU-labeled nuclei were located at the border, showing that replication sites were concentrated at the nuclear periphery. In some cells, labeling was seen only in the nucleus or only in the kinetoplast, but most cells were labeled in both the nucleus and the kinetoplast. The unlabeled area was larger than the nucleolus, as observed by DAPI staining, a finding also confirmed by confocal analysis (data not shown). When the cells were incubated with BrdU for 24 h, the labeling was found spread inside the nucleus, only excluding the nucleolar domain identified by the lack of DAPI staining (Fig. 1C). As indicated by [³H]thymidine incorporation (data not shown) and by cytometry analysis (see Fig. 5A), the S phase ended 8 to 10 h after HU release, and new nucleotide incorporation started only after 24 h. Therefore, these BrdU labeling experiments suggested that the replication sites were at the nuclear periphery and that replicated DNA moved to the nuclear interior during the progression of the cell cycle.

To confirm that the internal labeling corresponded to chromosomes that had moved and not to internal replication, HU-arrested cells were released, pulse-labeled with BrdU for 4 h, washed, and chased for additional periods of 4 and 20 h. After 4 h of chase, a period of time that correspond to the end of the

S phase, the labeling was still located at the periphery. In contrast, BrdU was found mainly inside the nucleus after 20 h of chasing (Fig. 1D), indicating that replicated chromosomes had moved to the interior when the cell cycle was completed. Figure 1E shows the mean intensity of labeling in a longitudinal section of several nuclei pulsed with BrdU for 4 and 20 h. From the diagram it was clear that the progression of the cell cycle resulted in signal dispersion throughout the nuclear space, excluding the nuclear periphery. These results also showed that the edge labeling was not due to antibody-limited access to the nuclear interior. The statistical analyses of these results are presented in Table 1; Student's *t* test showed that the alterations in BrdU localization were statistically significant.

Chromosome distribution in replicative epimastigote forms. To study chromosome localization in the nuclei of *T. cruzi*, we used satellite DNA as a probe in FISH assays. Satellite DNA sequences are present in 10 to 12 large chromosomes (1 to 3.5 Mbp) (4) (Fig. 2A) and form long clusters of about 200 repeats (30 kb); thus, they are suitable probes for monitoring a representative number of chromosomes. When exponentially growing epimastigotes were used, we found two patterns of hybridization. In half of the exponentially growing cells (*n* = 200), labeling was found as 10 to 12 dots organized at the nuclear periphery, while in the other half, it was found as dots randomly dispersed throughout the nuclear space (Fig. 2B). The number of dots matched the number of chromosomes containing the satellite repeats. The two labeling patterns observed were not due to different positions of parasite attachment to the glass slide, as they were seen throughout the fields at different focusing positions and, most importantly, were also observed in optical sections by confocal analysis. Figure 2C and D show representative images of optical sections of the peripheral and randomly dispersed patterns, respectively. From these images, it is clear that the peripheral labeling was present close to the entire nuclear envelope and that in the random pattern, the labeling was present in most of the nuclear space.

Next, we investigated whether these two labeling patterns
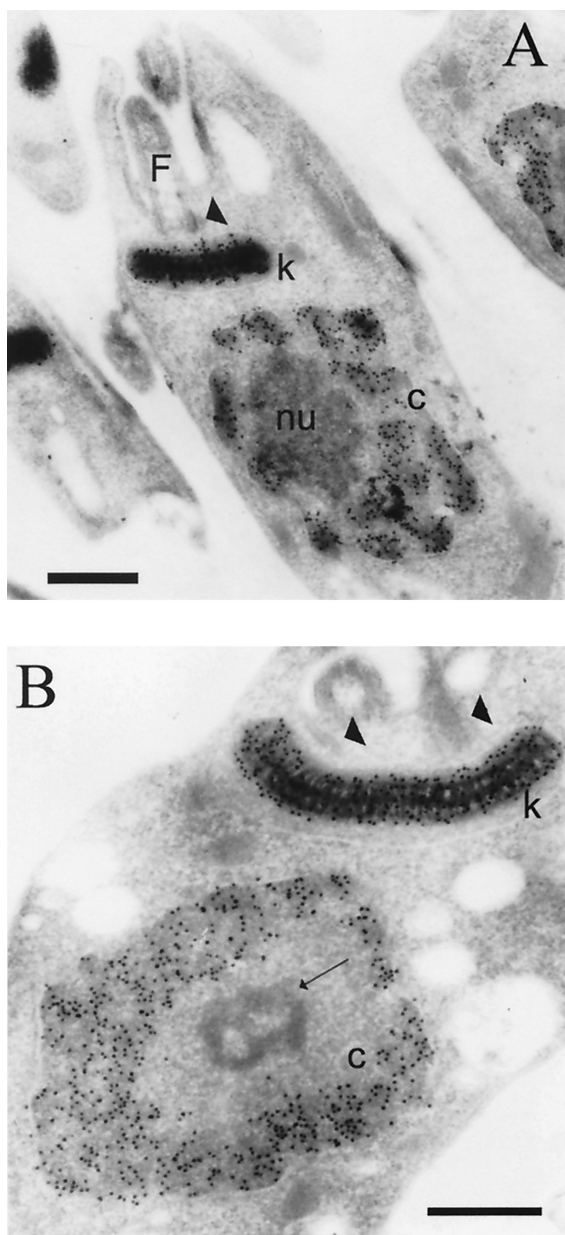
FIG. 4. Chromatin redistributes in epimastigote nuclei, as seen by electron microscopy. Thin sections of exponentially growing epimastigote forms were stained with TdT. (A) Interphase nucleus with intense colloidal gold labeling over the condensed masses of chromatin (C). The nucleolus (nu) can be identified as an electron-dense structure at the center of the nucleus. Note that this cell had only one flagellum (F), a single basal body (arrowhead), and a short kinetoplast (k), which may correspond to a cell in G_1. The nonreplicative kinetoplast was also labeled by the TdT technique. (B) Cell in S/G_2 phase. The DNA can be seen as dense structures (c) associated with the nuclear envelope. The nucleolus can be seen at the nuclear center (arrow). The kinetoplast is arch shaped, and two basal bodies (arrowheads) are present. Bars, 0.5 μm.

could be related to different phases of the cell cycle. Therefore, we studied the pattern of FISH signal distribution in epimastigotes simultaneously with the quantification of DNA by DAPI staining. Images were acquired at the same settings, and the total fluorescence intensity was quantified by using Qwin

software. The distribution of DAPI fluorescence intensity revealed two separate populations of cells showing the peripheral pattern and the dispersed pattern of FISH labeling with, respectively, high and low DAPI fluorescence intensities. An intermediate population of cells that could not be clearly separated was also present. The low DAPI labeling intensity corresponded to cells in the G_1 phase, intermediate labeling corresponded to the S phase, and strong labeling corresponded to the G_2 phase. As illustrated in Fig. 3A and B, parasites in the G_1 phase of the cell cycle had mainly chromosomes with the dispersed pattern. Parasites displaying more intense DAPI labeling corresponding to the S or G_2 phase had a high proportion of chromosomes distributed at the nuclear periphery. Cells in mitosis, identified by the presence of two nuclei and two arched kinetoplasts that appeared as two round structures with DAPI staining, showed chromosomes at the nuclear periphery but distributed at opposite poles. Finally, when mitosis was accomplished (parasites containing two nuclei and two elongated kinetoplasts), the staining started to disperse, resembling that found in the G_1 phase. That the chromosomes were dispersed first in one of the two nuclei when mitosis ended was a common observation. Of 29 G_1 images attributed to cells with a low level of DAPI staining, 18 displayed the random pattern and 11 displayed other patterns that did not include the typical peripheral pattern of S- or G_2-phase cells. Similarly, most of the S/G_2-, M-, and M/G_1-phase cells had the pattern of chromosome localization illustrated in Fig. 3B.

As the satellite distribution may represent a specific portion of the chromosomes, we investigated how DNA is distributed in the interphase nuclei of *T. cruzi*. Exponentially growing epimastigotes were fixed and sectioned for electron microscopy. The sections were then stained with BrdU triphosphate in the presence of TdT, a procedure that labels any DNA molecule (39). DNA nicks are generated by sectioning and occur at the surface of ultrathin sections. Cells in G_1 were identified by the presence of a shorter kinetoplast and just one basal body. The nucleolus was large compared to the nucleus, indicating a high level of transcriptional activity. In these cells, DNA was found mainly dispersed throughout the nuclear space, as shown by the colloidal gold staining in the TdT technique illustrated in Fig. 4A. Cells in S/G_2, identified by an arched kinetoplast and two basal bodies, showed DNA more concentrated at the nuclear periphery, excluding the nuclear interior (Fig. 4B). It is clear that DNA was excluded from a region surrounding a less electron-dense structure corresponding to the nucleolus. The nucleolus was not labeled in Fig. 4. However, in other sections, a low level of labeling of the nucleolus could be clearly seen (data not shown), indicating that this central area of the nucleus contains very little DNA.

Chromosomes are constrained at the nuclear periphery at the onset of the S phase. Since we have shown that chromosome localization is related to the cell cycle, we investigated the position of the satellite probe in HU-arrested cells. Epimastigotes maintained in cultures in the presence of HU for 24 h were labeled with propidium iodide and subjected to flow cytometry analysis. These cells appeared as a single population containing amounts of DNA corresponding to the G_1 phase, compatible with cells arrested before DNA duplication (early S phase), while control cells showed two peaks corresponding to cells in G_1 and G_2 (Fig. 5A). Analysis of the same cells by FISH
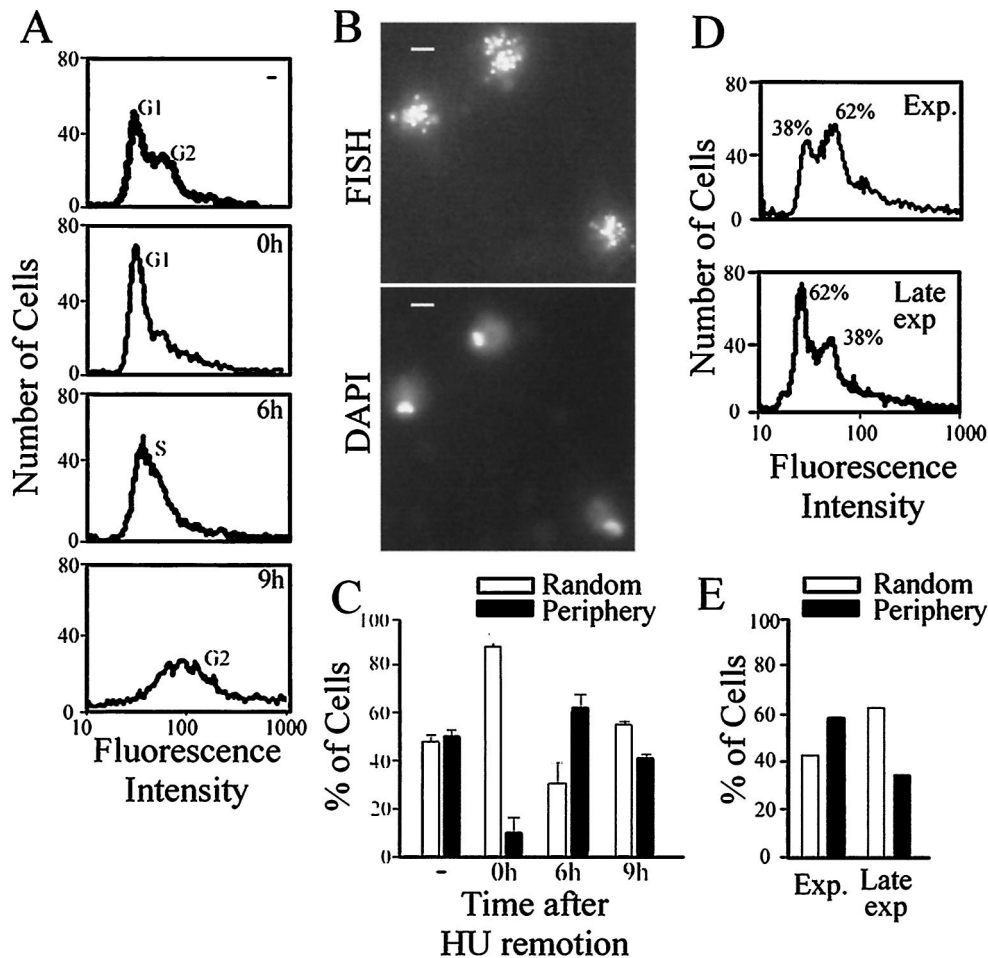
FIG. 5. Chromosomes relocate to the nuclear periphery during the cell cycle. (A) Flow cytometry analysis of propidium iodide-stained epimastigotes that were not treated (−) or treated with 20 mM HU for 24 h, washed, and kept in cultures for the indicated times (0, 6, and 9 h). (B) FISH images of epimastigotes treated with HU and probed with the satellite repeat sequence. Note that most of the labeling was found randomly in the nuclear space. Bars, 1 μm. (C) Quantitative analysis of the patterns of chromosome localization seen in control cells or cells released from HU treatment for the indicated times. Each bar represents the mean and standard deviation of three independent experiments for dots randomly distributed or located in the nuclear periphery. (D) Flow cytometry analysis of exponentially growing (Exp.) or late-exponential-phase (Late exp) epimastigote cultures labeled with propidium iodide. The numbers above the peaks correspond to the percentages of cells containing the indicated fluorescence. (E) Quantitative FISH analysis of the samples shown in panel D.

with satellite DNA as a probe revealed that HU-treated parasites had the pattern found in G_1 for nonsynchronized cells, with labeling localized randomly in the nuclear space in more than 90% of the cells (Fig. 5B and C). From 3 to 6 h after HU removal, a large proportion of cells entered the S phase and more than 65% showed satellite labeling at the nuclear edge (Fig. 5C), indicating that the chromosomes were constrained at the nuclear periphery during the S phase. After longer incubation times (9 h), cytometry analysis showed a pattern of fluorescence compatible with cells in G_2. In the latter situation, the number of cells containing satellite DNA labeling in the nuclear interior increased.

To exclude the possibility that an unexpected HU effect interfered with chromosome distribution, we checked the chromosome localizations of exponential-phase and late-exponential-phase cell cultures, in which most of the cells were no longer growing. In a typical experiment, 38% of the parasites in the exponential growth phase contained DNA amounts equiv-

alent to the G_1 phase and 62% contained DNA amounts equivalent to the S/G_2 phase, as detected by cytometry analysis, while in late-exponential-phase cultures, the numbers were the opposite (Fig. 5D). In exponential-phase cultures, we consistently found more parasites with chromosomes labeled at the nuclear edge, while in late-exponential-phase cultures, there were more parasites with the random labeling pattern (Fig. 5E); these results indicated that the dispersed labeling pattern predominated in naturally arrested G_1-phase cells. These results indicate that satellite localization is related to replication status, with chromosomes being constrained at the nuclear periphery for replication to occur and being dispersed into the nuclear interior after cell division.

Chromosomes are dispersed inside the nuclear space of nonreplicative trypomastigote forms. The life cycle of *T. cruzi* alternates replicative and noninfective forms with nonreplicative and infective forms. Since our results showed that the chromosome distribution was related to the replication pro-
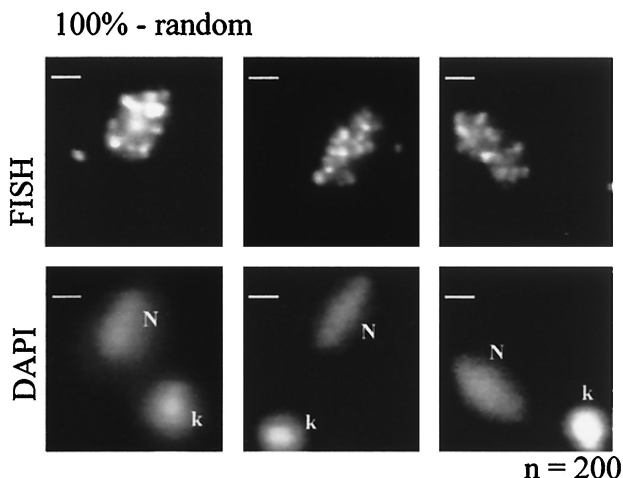
100% - random

FIG. 6. Nonreplicative trypomastigote forms with chromosomes randomly dispersed in the nucleus. The satellite probe labeled with digoxigenin was used to probe cell-derived trypomastigotes. The images show representative examples of FISH and DAPI staining. The number above the images corresponds to the percentage of the pattern observed (random) in 200 cells. N, nucleus; k, kinetoplast. Bars, 1 μm.

cess, we investigated the localization of chromosomes in non-replicative trypomastigote forms. A FISH assay with trypomastigotes showed that 100% of the parasites had chromosomes randomly dispersed in the nucleus (Fig. 6). This result confirms that the peripheral pattern, a consequence of chromosome movement, is indeed related to DNA replication.

DISCUSSION

In the present study, we showed that the localization of chromosomes changes in *T. cruzi* nuclei according to the cell cycle. The satellite sequences, which represent 10% of the parasite genome and are repeated clusters of 195 bp found in
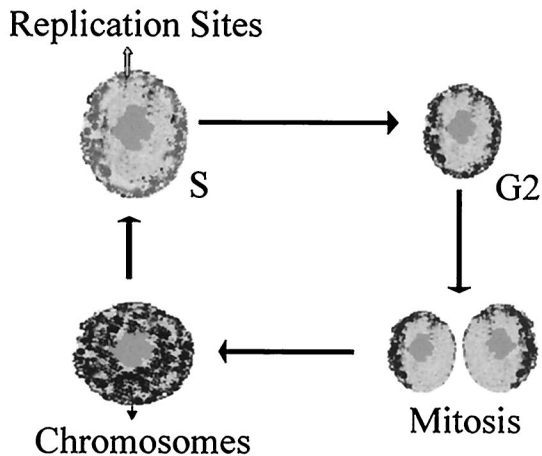

FIG. 7. Model of chromosome dynamics during the cell cycle of *T. cruzi*. At the G$_1$ phase, chromosomes are found dispersed in the nucleus. During the replicative stage of the cell cycle, the chromosomes are retained at the nuclear periphery, staying at opposite poles during mitosis and dispersing when mitosis is completed. Nucleolar components are located in the center of the structures.

most of the large parasite chromosomes, are mainly distributed in the nuclear interior in nonreplicating stages and in cells in the G$_1$ phase of the cell cycle. At the beginning of the S phase, these sequences are found at the nuclear periphery, which contains most of the replication sites, as determined by BrdU labeling. Therefore, these positional changes indicate that *T. cruzi* chromosomes move during the cell cycle and replicate at the nuclear periphery, as illustrated in Fig. 7.

Several experimental results showed that *T. cruzi* chromosomes are distributed differently at the sequential stages of the cell cycle. In exponentially growing epimastigotes, most of the parasites are replicating and most of the FISH labeling is detected at the nuclear periphery. Most importantly, a high correlation is seen between a peripheral distribution in cells and a large amount of DAPI labeling. In contrast, a random distribution throughout the nuclear space is seen in late-exponential-phase cultures (which contain nonreplicating cells), in cells in the G$_1$ phase (identified by the low level of labeling with DAPI), in HU-arrested cells, and in infective and differentiated forms. Optical sectioning demonstrated that the peripheral FISH labeling surrounds the nuclear compartment and that the random labeling corresponds to chromosomes dispersed throughout the entire nuclear compartment. In addition, our results reinforce the notion that both patterns may exist in live cells and are not the consequence of chromosome spreading or parasite flattening during fixation. Besides, trypomastigotes, which are nonreplicating forms arrested in a G$_0$-like stage, consistently showed labeling in a dispersed pattern.

The fact that we used a repeated DNA sequence as a probe could reflect the dynamics of particular regions but not of the entire chromosome. The 195-bp sequence is proportionally less transcribed in *T. cruzi* (9), and it is not located near telomeres, as indicated by *Bal* 31 digestion of intact chromosomes (33). It could play a role in chromosome segregation, behaving like other centromeric or heterochromatic sequences, which show occasional changes in chromosome positions during interphase (34). Moreover, it has been shown that repeated sequences form heterochromatin that replicates at later times of the S phase and is preferentially localized at the nuclear periphery in other eukaryotes (25–27, 43). Therefore, in the present study, chromosome localization at the nuclear periphery could have occurred preferentially for the satellite DNA. Nevertheless, the finding that BrdU staining occupies a much larger area in *T. cruzi* nuclei than does that of satellite hybridization argues in favor of the idea that other chromosome sequences may be localized at the nuclear periphery along with the satellite repeats. In addition, DNA labeling of thin sections also revealed that all chromatin in S/G$_2$-phase cells was more concentrated toward the surface of nuclei. The fact that DAPI stained most of the nucleus could argue that DNA is present in the entire nuclear space. However, the DAPI signal was quite dispersed and did not allow precise DNA localization with a regular fluorescence microscope. In fact, the electron microscopy images showed clearly major chromatin redistribution after the beginning of the S phase; this finding was not due to nucleolar expansion, as the size of the nucleolus seems to be reduced when DNA is located at the periphery.

We localized replication sites either after cell synchronization in the presence of HU or in nonsynchronized cells. Since HU arrests cells at the beginning of the S phase, it is possible

that at this point, genes that replicate early had already been triggered, and the BrdU incorporation observed could have been due to the replication of genes that replicate late. In *T. cruzi*, HU arrests cell growth and replication (14), but the precise mechanism by which it acts is not well known. At the earliest times at which we could detect the BrdU signal in nonsynchronized cells, all labeling was found at the periphery. Similarly, the incorporation of BrdU after HU arrest labeled the nuclear periphery. With long incubations or a BrdU chase, the labeling was dispersed, reinforcing the notion that replicated chromosomes are redistributed toward the nuclear interior after completion of the cell cycle. The precise locations of replication sites at the beginning of the S phase could not be determined because, under our conditions, BrdU labeling was not detected by short pulses after HU release. We could detect only diffuse labeling in the cytoplasm (possibly in the mitochondria) with short incubation times. Nevertheless, these labeling kinetics are similar to those of [³H]thymidine incorporation into DNA, which shows a lag of about 2 h. A similar recovery from the HU block has also been observed in *T. brucei* (30). It is possible that thymidine phosphorylase converts BrdU to bromouracil, as in *Crithidia* (35), impairing labeling. Moreover, the failure to detect BrdU labeling with short incubation times might have occurred because we could label *T. cruzi* only in a rich medium, and the presence of nucleotides in this medium could have affected BrdU incorporation.

The movement of chromosomes was clearly seen in the long BrdU incubation and chase experiments, as the labeling in these experiments was found in the nuclear interior. The possibility that labeling occurred in the nuclear interior is unlikely, because (i) the S phase ends at 8 to 10 h after HU release (Fig. 5A), (ii) thymidine incorporation also ceases after 8 to 10 h (data not shown) (14), and (iii) a new replication cycle starts only after 24 h. The molecular mechanism involved in chromosome dynamics is unknown. It is possible that a set of unknown proteins is able to constrain chromosomes at replication sites during the S phase. These effects could be mediated by proteins like heterochromatin binding protein HP1, known to interact with the replication origin complexes at replication origins in DNA (5) and with the internal nuclear membrane (41). These effects could be mediated by histone acetylation, which would release the HP1-like protein, as in other cells (37); methylation would increase the binding of HP1 to chromatin and the formation of heterochromatin (2, 23), affecting the positions of chromosomes in the nucleus.

As recently described for yeast cells (18), chromosome redistribution can be explained by the fact that chromosomes are continuously moving but become immobilized at the nuclear periphery in the S phase via the interaction with the replication machinery. Alternatively, the chromosomes in *T. cruzi* could be dispersed in the nuclear space, moving to the periphery only when they replicate. The present results do not allow us to discriminate between these two hypotheses, but they are consistent with the proposal that at least some of the chromosome dynamics inside the nucleus are related to movement toward "fixed" replication sites (22), as in other eukaryotes (19). Recent studies with yeast and mammalian cells revealed that the positioning of a gene in the nucleus is thought to regulate its transcriptional state (17) and that chromosome territories are determined by a transcriptional gradient (32). The lack of selective transcriptional control in trypanosomes, as well as the present findings, suggests that chromosome localization is dictated mainly by the cell cycle and/or replication control in *T. cruzi*.

REFERENCES

1. **Abuin, G., L. H. G. Freitas-Junior, W. Colli, M. J. Alves, and S. Schenkman.** 1999. Expression of *trans*-sialidase and 85 kDa glycoprotein genes in *Trypanosoma cruzi* is differentially regulated at the post-transcriptional level by labile protein factors. J. Biol. Chem. **274:**13041–13047.
2. **Bannister, A. J., P. Zegerman, J. F. Partridge, E. A. Miska, J. O. Thomas, R. C. Allshire, and T. Kouzarides.** 2001. Selective recognition of methylated lysine 9 on histone H3 by the HP1 chromo domain. Nature **410:**120–124.
3. **Camargo, E. P.** 1964. Growth and differentiation in *Trypanosoma cruzi*: origin of metacyclic trypomastigotes in liquid media. Rev. Inst. Med. Trop. Sao Paulo **6:**93–100.
4. **Cano, M. I., A. Gruber, M. Vazquez, A. Cortés, M. J. Levin, A. Gonzalez, W. Degrave, E. Rondinelli, B. Zingales, J. L. Ramirez, C. Alonso, J. M. Requena, and J. F. Da Silveira.** 1995. Molecular karyotype of clone CL Brener chosen for the *Trypanosoma cruzi* genome project. Mol. Biochem. Parasitol. **71:**273–278.
5. **Cavalli, G., and R. Paro.** 1998. Chromo-domain proteins: linking chromatin structure to epigenetic regulation. Curr. Opin. Cell Biol. **10:**354–360.
6. **Cremer, T., G. Kreth, H. Koester, R. H. Fink, R. Heintzmann, M. Cremer, I. Solovei, D. Zink, and C. Cremer.** 2000. Chromosome territories, interchromatin domain compartment, and nuclear matrix: an integrated view of the functional nuclear architecture. Crit. Rev. Eukaryot. Gene Expr. **10:**179–212.
7. **DePamphilis, M. L.** 2000. Review: nuclear structure and DNA replication. J. Struct. Biol. **129:**186–197.
8. **Dundr, M., and T. Misteli.** 2001. Functional architecture in the cell nucleus. Biochem. J. **356:**297–310.
9. **Elias, M. C., R. Marques-Porto, E. Freymuller, and S. Schenkman.** 2001. Transcription rate modulation through the *Trypanosoma cruzi* life cycle occurs in parallel with changes in nuclear organisation. Mol. Biochem. Parasitol. **112:**79–90.
10. **Ferguson, M., and D. C. Ward.** 1992. Cell cycle dependent chromosomal movement in pre-mitotic human T-lymphocyte nuclei. Chromosoma **101:**557–565.
11. **Ferreira, J., G. Paolella, C. Ramos, and A. I. Lamond.** 1997. Spatial organization of large-scale chromatin domains in the nucleus: a magnified view of single chromosome territories. J. Cell Biol. **139:**1597–1610.
12. **Filho, S. A., E. R. Pereira de Almeida, and E. S. Gander.** 1978. The influence of hydroxyurea and colchicine on growth and morphology of *Trypanosoma cruzi*. Acta Trop. **35:**229–237.
13. **Freitas-Junior, L. H., R. M. Porto, L. A. Pirrit, S. Schenkman, and A. Scherf.** 1999. Identification of the telomere in *Trypanosoma cruzi* reveals highly heterogeneous telomere lengths in different parasite strains. Nucleic Acids Res. **27:**2451–2456.
14. **Galanti, N., J. A. Dvorak, J. Grenet, and J. P. McDaniel.** 1994. Hydroxyurea-induced synchrony of DNA replication in the Kinetoplastida. Exp. Cell Res. **214:**225–230.
15. **Gonzalez, A., E. Prediger, M. E. Huecas, N. Nogueira, and P. M. Lizardi.** 1984. Minichromosomal repetitive DNA in *Trypanosoma cruzi*: its use in a high-sensitivity parasite detection assay. Proc. Natl. Acad. Sci. USA **81:**3356–3360.
16. **Gunawardena, S., and M. C. Rykowski.** 2000. Direct evidence for interphase chromosome movement during the mid-blastula transition in *Drosophila*. Curr. Biol. **10:**285–288.
17. **Hediger, F., and S. M. Gasser.** 2002. Nuclear organization and silencing: putting things in their place. Nat. Cell Biol. **4:**E53-E55.
18. **Heun, P., T. Laroche, K. Shimada, P. Furrer, and S. M. Gasser.** 2001. Chromosome dynamics in the yeast interphase nucleus. Science **294:**2181–2186.
19. **Heun, P., A. Taddei, and S. M. Gasser.** 2001. From snapshots to moving pictures: new perspectives on nuclear organization. Trends Cell Biol. **11:**519–525.
20. **Hofer, A., J. T. Ekanem, and L. Thelander.** 1998. Allosteric regulation of

Trypanosoma brucei ribonucleotide reductase studied in vitro and in vivo. J. Biol. Chem. **273:**34098–34104.

21. **Hotz, H. R., S. Biebinger, J. Flaspohler, and C. Clayton.** 1998. PARP gene expression: control at many levels. Mol. Biochem. Parasitol. **91:**131–143.

22. **Hozak, P., A. B. Hassan, D. A. Jackson, and P. R. Cook.** 1993. Visualization of replication factories attached to nucleoskeleton. Cell **73:**361–373.

23. **Lachner, M., D. O'Carroll, S. Rea, K. Mechtler, and T. Jenuwein.** 2001. Methylation of histone H3 lysine 9 creates a binding site for HP1 proteins. Nature **410:**116–120.

24. **Lamond, A. I., and W. C. Earnshaw.** 1998. Structure and function in the nucleus. Science **280:**547–553.

25. **Leonhardt, H., H. P. Rahn, P. Weinzierl, A. Sporbert, T. Cremer, D. Zink, and M. C. Cardoso.** 2000. Dynamics of DNA replication factories in living cells. J. Cell Biol. **149:**271–280.

26. **Li, G., G. Sudlow, and A. S. Belmont.** 1998. Interphase cell cycle dynamics of a late-replicating, heterochromatic homogeneously staining region: precise choreography of condensation/decondensation and nuclear positioning. J. Cell Biol. **140:**975–989.

27. **Ma, H., J. Samarabandu, R. S. Devdhar, R. Acharya, P. C. Cheng, C. Meng, and R. Berezney.** 1998. Spatial and temporal dynamics of DNA replication sites in mammalian cells. J. Cell Biol. **143:**1415–1425.

28. **Ma, H., A. J. Siegel, and R. Berezney.** 1999. Association of chromosome territories with the nuclear matrix. Disruption of human chromosome territories correlates with the release of a subset of nuclear matrix proteins. J. Cell Biol. **146:**531–542.

29. **Moir, R. D., T. P. Spann, H. Herrmann, and R. D. Goldman.** 2000. Disruption of nuclear lamin organization blocks the elongation phase of DNA replication. J. Cell Biol. **149:**1179–1192.

30. **Morgan, G. A., E. A. Hamilton, and S. J. Black.** 1996. The requirements for G1 checkpoint progression of *Trypanosoma brucei* S 427 clone 1. Mol. Biochem. Parasitol. **78:**195–207.

31. **Nakamura, H., T. Morita, and C. Sato.** 1986. Structural organizations of replicon domains during DNA synthetic phase in the mammalian nucleus. Exp. Cell Res. **165:**291–297.

32. **Sadoni, N., S. Langer, C. Fauth, G. Bernardi, T. Cremer, B. M. Turner, and D. Zink.** 1999. Nuclear organization of mammalian genomes. Polar chromosome territories build up functionally distinct higher order compartments. J. Cell Biol. **146:**1211–1226.

33. **Santos, M. R., H. Lorenzi, P. Porcile, M. S. Carmo, A. Schijman, A. Brandao, J. E. Araya, H. B. Gomes, M. A. Chiurillo, J. L. Ramirez, W. M. Degrave, M. J. Levin, and J. F. Da Silveira.** 1999. Physical mapping of a 670-kb region of chromosomes XVI and XVII from the human protozoan parasite *Trypanosoma cruzi* encompassing the genes for two immunodominant antigens. Genome Res. **9:**1268–1276.

34. **Shelby, R. D., K. M. Hahn, and K. F. Sullivan.** 1996. Dynamic elastic behavior of alpha-satellite DNA domains visualized in situ in living human cells. J. Cell Biol. **135:**545–557.

35. **Simpson, A. M., and L. Simpson.** 1974. Labeling of *Crithidia fasciculata* DNA with (^{3}H)thymidine. J. Protozool. **21:**379–382.

36. **Spector, D. L.** 1993. Macromolecular domains within the cell nucleus. Annu. Rev. Cell Biol. **9:**265–315.

37. **Taddei, A., C. Maison, D. Roche, and G. Almouzni.** 2001. Reversible disruption of pericentric heterochromatin and centromere function by inhibiting deacetylases. Nat. Cell Biol. **3:**114–120.

38. **Teixeira, S. M.** 1998. Control of gene expression in Trypanosomatidae. Braz. J. Med. Biol. Res. **31:**1503–1516.

39. **Thiry, M.** 1992. Highly sensitive immunodetection of DNA on sections with exogenous terminal deoxynucleotidyl transferase and non-isotopic nucleotide analogues. J. Histochem. Cytochem. **40:**411–419.

40. **Woodward, R., and K. Gull.** 1990. Timing of nuclear and kinetoplast DNA replication and early morphological events in the cell cycle of *Trypanosoma brucei*. J. Cell Sci. **95:**49–57.

41. **Ye, Q., I. Callebaut, A. Pezhman, J. C. Courvalin, and H. J. Worman.** 1997. Domain-specific interactions of human HP1-type chromodomain proteins and inner nuclear membrane protein LBR. J. Biol. Chem. **272:**14983–14989.

42. **Young, C. W., G. Schochetman, S. Hodas, and M. E. Balis.** 1967. Inhibition of DNA synthesis by hydroxyurea: structure-activity relationships. Cancer Res. **27:**535–540.

43. **Zink, D., H. Bornfleth, A. Visser, C. Cremer, and T. Cremer.** 1999. Organization of early and late replicating DNA in human chromosome territories. Exp. Cell Res. **247:**176–188.